



1 **Comparison of flux gradient and chamber techniques to measure soil N₂O emissions**

2 Mei Bai^{1,*}, Helen Suter¹, Shu Kee Lam¹, Thomas K. Flesch², Deli Chen¹

3 ¹Faculty of Veterinary and Agricultural Sciences, The University of Melbourne, Parkville, VIC

4 3010, Australia

5 ²Department of Earth and Atmospheric Sciences, University of Alberta, Edmonton, AB T6G

6 2R3, Canada

7 *Correspondence to:* Mei Bai (mei.bai@unimelb.edu.au)

8

9 **Abstract**

10 Improving the direct field measurement techniques to quantify gases emissions from the large
11 agriculture farm is challenging. We compared nitrous oxide (N₂O) emissions measured with
12 static chambers to those from a newly developed micrometeorological flux gradient (FG)
13 approach. Measurements were made at a vegetable farm following chicken manure application.
14 The FG calculations were made with a single open-path Fourier transform infrared (OP-FTIR)
15 spectrometer (height of 1.45 m) deployed in a slant-path configuration: sequentially aimed at
16 retro reflectors at heights of 0.8 and 1.8 m above ground. Hourly emissions were measured
17 with the FG technique, but once a day between 10:00 and 13:00 with chambers. We compared
18 the concurrent emission ratios (FG/Chambers) between these two techniques, and found N₂O
19 emission rates from celery crop farm measured at mid-day by FG were statistically higher (1.4
20 times) than those from the chambers measured at the same time. Our results suggest the OP-
21 FTIR slant-path FG configuration worked well in this study: it was sufficiently sensitive to
22 detect the N₂O gradients over our site, giving high temporal resolution N₂O emissions
23 corresponding to a large measurement footprint.

24



25 **Keywords:** chamber techniques, chicken manure, flux gradient, N₂O emission, OP-FTIR
26 spectroscopy

27

28 **Abbreviations:** FG, flux gradient; OP-FTIR, open-path Fourier transform infrared
29 spectroscopy

30

31 **1 Introduction**

32 The accurate measurement of soil nitrous oxide (N₂O) emissions from agricultural land is
33 challenging. Chambers are commonly used for these measurements (Hutchinson and Mosier,
34 1981), and chamber based observations are widely used to calculate greenhouse gas inventories
35 (Dalal et al., 2008). The principle behind the most common type of chamber measurement
36 (static, or non-steady state) is to create a sealed control volume over the soil surface, such that
37 by monitoring the gas concentration change during the chamber deployment, one can calculate
38 the surface emission rate (Denmead, 2008). One of the advantages of chambers is that they can
39 be employed at relatively low cost, with simplicity and easy field operation (de Klein et al.,
40 2001). However, chambers have a fundamental limitation – the control volume inevitably
41 perturbs the soil-atmosphere interface (e.g., temperature, pressure), which has the potential to
42 modify the ambient soil emission rate (Denmead, 1979). Moreover, static chambers are not
43 well-suited to measure temporal variations in emissions (Denmead et al., 2008; Jones et al.,
44 2011). These weaknesses can be addressed by alternative approaches, e.g. a dynamic
45 measurement with automated-chamber opening and closing by pneumatic actuators (Yao et al.,
46 2009) and can be run for many months. However, in many situations the most important
47 disadvantage of chambers is their small surface measurement footprint. With a surface
48 enclosure typically less than 1 m², and the likelihood that soil emissions vary dramatically at
49 length scales greater than 1 m (Denmead, 2008; Griffith and Galle, 2000; Turner et al., 2008),



50 many replications are needed to adequately quantify the emissions from an agricultural field
51 (Christensen et al., 1996; Denmead, 1995).

52

53 Micrometeorological measurements avoid some of the problems associated with chamber
54 methods (Christensen et al., 1996; Denmead et al., 2010; Li et al., 2008; Pattey et al., 2006).

55 These techniques are based on concentration and windflow measurements made in the free air
56 above the surface, and they do not perturb the surface environment. They also measure
57 emissions over footprints much larger than those from chambers (Hargreaves et al., 1996). The

58 flux gradient (FG) technique is a well-used micrometeorological method, where the vertical
59 flux of gas is inferred from a height gradient in concentration (multiplied by an estimate of the
60 gas diffusivity). When measured above a large and homogeneous surface, this atmospheric flux

61 is assumed equal to the underlying surface emission or absorption rate. In this study we used a
62 recently developed modification of the technique. Rather than vertically separated point
63 concentrations, we used a slant-path configuration based on vertically separated long line-

64 averaged measurements (Flesch et al., 2016; Wilson and Flesch, 2016). A single open-path
65 Fourier transform infrared (OP-FTIR) concentration sensor with motorized aiming gives the
66 gas concentrations along the two paths, from which we can calculate the surface

67 emission/deposition rate.

68

69 In this study we conducted a set of N₂O emission measurements from a vegetable farm
70 following manure application. Measurements were made with both static chambers and the
71 slant-path FG approach. Our objective was to 1) demonstrate the newly developed slant-path

72 FG method at a vegetable farm; and 2) compare the emission rates measured by the static
73 chamber and FG techniques.

74



75 **2 Materials and methods**

76 **2.1 Experimental site**

77 This study was conducted at an intensive vegetable farm in Clyde, Victoria, Australia (38.1°
78 S, 145.3° E). The site consisted of two adjacent fields of 5.4 ha (Site 1) and 3.1 ha (Site 2).
79 These sites differ only in the addition of a fertilizer amendment at Site 2. A celery crop at the
80 4-5 leaf stage was transplanted to these two sites on 27 February 2014 (Fig. 1). Chicken manure
81 (4.3% N, $\text{NH}_4^+\text{-N}$: 4633 mg kg⁻¹, $\text{NO}_3\text{-N}$: 313 mg kg⁻¹) was applied at rate of 8.2 tonne ha⁻¹ at
82 both sites on 28 March. Fertiliser Cal-Gran (a blend of calcium ammonium nitrate and
83 ammonium sulphate, total 23.9% N) was also applied at both sites at rate of 200 kg ha⁻¹ on 15
84 April. Emission measurements began just prior to manure application and ended on 6 May
85 2014. The terrain was open and flat with sandy loam topsoils. Prevailing winds were southeast
86 or northwest during this period. The average minimum and maximum temperature was 6 and
87 33°C, respectively. The total precipitation (including rainfall and irrigation) during the
88 measurement period was 186 mm.

89 Figure 1

90

91 **2.2 Methodologies**

92 **2.2.1 Static chamber**

93 Four static chambers (50 × 50 × 25 cm) were located at each site (Fig. 1). The metal base for
94 each chamber was placed into the soil to a depth of 8 cm prior to the experiment, and remained
95 in place through the study. The chamber was made of plexiglass with a built in ventilation
96 system. Reflective aluminium foil was attached inside the lid to minimize changes in ambient
97 pressure and temperature after the chamber was placed onto the base. A thermocouple Tinytag
98 Transit 2 (TG-4080 temperature loggers, West Sussex, UK) was placed on the soil surface
99 inside the chamber to monitor the headspace air temperature. Gas samples (20 mL) were



100 collected into evacuated 12 mL vials (Exetainer®, Labco Ltd., Ceredigion, UK) at 0, 30 and
101 60 minutes after chamber placement and analysed at an off-site laboratory by gas
102 chromatography (GC) (Agilent 7890A, Wilmington, USA). The sensitivity of GC for N₂O
103 concentration was 0.01 ppm. Gas samples were collected daily between 10:00 and 13:00 from
104 29 March to 7 April and on 9, 11 and 16 April. The N₂O flux was calculated as (Ruser et al.,
105 1998) (Eq. 1):

$$106 \quad Q_{chamber} = \kappa (273/T) (V/A) dC/dt \quad (1)$$

107 where $Q_{chamber}$ is the gas flux ($\mu\text{g N}_2\text{O-N m}^{-2} \text{h}^{-1}$), κ is a density factor for N₂O gas, 1.25 (μg
108 $\text{N } \mu\text{L}^{-1}$), T is the air temperature within the chamber (K), V is the total volume of headspace
109 (L), A is a surface area inside the chamber (m^2), dC/dt is the rate of change in concentration of
110 N₂O in the chamber ($\mu\text{L L}^{-1} \text{h}^{-1}$).

111

112 2.2.2 Flux gradient

113 The basic principle of the FG method has been well-described (Judd et al., 1999; Laubach and
114 Kelliher, 2004; Webb et al., 1980). We followed a modification described in Flesch et al.
115 (2016), in which an open-path sensor was used to measure the concentration difference (ΔC_L)
116 between two slant-paths. The open-path sensor measures gas concentration between the sensor
117 and a distant retro reflector. The concentration difference ΔC_L is calculated by sequentially
118 aiming the sensor at high and low retro reflectors (Eqs. 2, 3):

$$119 \quad Q_{FG} = (k_v \rho_a u^* / S_c) (M_s / M_a) * \kappa * \Delta C_L \quad (2)$$

$$120 \quad \kappa = l_{PATH} / \int_{x_1}^{x_2} [\ln(z_{p2} / z_{p1}) - \phi(z_{p2}/L) + \phi(z_{p1}/L)] dx \quad (3)$$

121 where Q_{FG} is the gas flux ($\text{g m}^{-2} \text{s}^{-1}$), k_v is von Karman's constant (0.4), ρ_a is dry air density (g
122 m^{-3}), u^* is friction velocity (m s^{-1}), S_c is the turbulent Schmidt number (0.64), M_s and M_a are
123 the molar mass of N₂O (44 g mol^{-1}) and dry air (29 g mol^{-1}), respectively, ΔC_L (ppb) is the



124 difference in the line-average volumetric mixing ratio of the gas (relative to dry air) from the
125 lower (z_{p1}) and upper (z_{p2}) paths (m, relative to celery beds surface), κ is proportional to the
126 height integral of the gas diffusivity along the FTIR path pair, l_{PATH} is the sensor-retro reflector
127 path length (m, equal for the two paths), L is atmospheric Obukhov stability length (m). Path
128 heights (z_{p1} and z_{p2}) along the path length are given by a 5th-order polynomial fit of height vs.
129 distance from the OP-FTIR spectrometer (path heights were measured in the field at 5 m
130 intervals). We used the stability correction factor φ from Flesch et al. (2016).

131

132 An estimate of the uncertainty in Q_{FG} (δQ_{FG}) was calculated as the sum in quadrature of the
133 relative uncertainties in S_c , ΔCL and κ according to the formula described in Flesch et al. (2016).
134 Q_{FG} values were not calculated when $u^* < 0.05 \text{ m s}^{-1}$.

135

136 The FG calculations relied on open-path concentrations measured with a robust Bruker OP-
137 FTIR spectrometer (Matrix-M IRcube, Bruker Optics, Ettlingen, Germany) and two retro
138 reflectors located 80 m from the spectrometer (PLX Industries, New York, USA). Briefly, the
139 OP-FTIR system measures multiple gas concentrations (N_2O , CH_4 , NH_3 , CO_2 , CO and water
140 vapour) with high precision (Griffith, 1996; Griffith et al., 2012). More details on the OP-FTIR
141 system can be found in Bai (2010). The spectrometer was mounted at a height of 1.45 m above
142 ground. A motorized mounting head sequentially aimed the spectrometer to the retro reflectors
143 at 0.8 and 1.8 m above ground. Line-averaged N_2O concentrations with an averaging time of
144 2.5-min were measured. Background concentrations prior to manure application were
145 averaged, the standard deviation of the mean was retrieved and the precision of N_2O
146 concentration measurements (less than 0.3 ppb) was determined according to Bai (2010). The
147 OP-FTIR measurements were made continuously from 25 March until 16 April, and thereafter
148 measurements were made for three days (continuously) per week until 6 May.



149

150 A weather station coupled with a three-dimensional sonic anemometer (CSAT3, Campbell
151 Scientific, Logan, UT, USA) was established at a height of 3.0 m above ground, 50 m east of
152 Site 2. Fifteen-min average climatic data including ambient temperature, pressure and wind
153 statistics were recorded by a data logger (CR23X, Campbell Scientific, Logan, UT, USA) at
154 frequency of 10 Hz. Atmospheric stability parameters of friction velocity (u^*), surface
155 roughness (z_0) and Obukhov stability length (L) were calculated. We used a data filtering
156 procedure to remove error-prone observations in the FG calculation according to Flesch et al.
157 (2014).

158 To compare the two measurement techniques we looked at periods with concurrent
159 measurements from FG and the chambers, and hourly flux ratios of $Q_{FG}/Q_{chamber}$ measured
160 between 10:00 and 13:00 are compared.

161

162 **3 Results and discussion**

163 **3.1 Daily N₂O flux**

164 The FG measurements gave high temporal resolution of fluxes and this provides an opportunity
165 to study the pattern of N₂O emissions in detail. Here we only describe the temporal flux
166 measurements from Site 1.

167

168 **3.1.1 The FG fluxes**

169 Hourly N₂O fluxes showed large temporal variation during the experimental period in response
170 to fertilisation. There was a rapid increase in N₂O emission from a background level of 0.6 mg
171 N₂O–N m⁻² h⁻¹ before manure application to a peak of 158.0 mg N₂O–N m⁻² h⁻¹ within 24 h
172 after application, which could be attributed to both nitrification and denitrification. After the
173 peak, several spikes between 16–17 April were also observed associated with fertilizer



174 application, followed by a decline in emissions to an average of $2.5 \text{ mg N}_2\text{O-N m}^{-2} \text{ h}^{-1}$ (Fig.
175 2A). One of the conclusions we draw from Figure 2B is that the slant path FG system is
176 sensitive enough to measure the N_2O fluxes that accompanied fertilisation at our site, i.e., the
177 measurement uncertainty as represented by $1-\sigma$ is generally well below the flux magnitude.

178

179 In addition to the long-term pattern of decreasing emissions after manure application, we
180 observed a diurnal pattern where maximum emission tended to occur in the late afternoon
181 (16:00) (Fig. 2B). We believe this is related to the time of maximum soil surface temperature,
182 which occurs after the peak air temperature (Christensen et al., 1996; Wang et al., 2013). A
183 strong diurnal emission pattern implies that once-a-day snapshot emission measurements (e.g.,
184 chambers) would almost certainly give a biased estimate of the daily average emission rate.
185 We also noticed occasional high emissions at night, which was closely related to precipitation
186 events. Negative N_2O fluxes calculated from the FG measurements most likely represent
187 instrument noise, as the flux magnitudes were below the detectable limit of our OP-FTIR
188 system, e.g., the uncertainty represented by the $1-\sigma$ error bars in Fig. 2 span zero.

189 Figure 2

190

191 3.1.2 Chamber fluxes

192 Nitrous oxide fluxes from the static chambers (once-a-day snapshots) were in general
193 agreement with the FG measurements in terms of the long-term pattern (Fig. 2): hourly fluxes
194 rose from a background level of $1.12 \text{ mg N}_2\text{O-N m}^{-2} \text{ h}^{-1}$ (before manure application, data is
195 not shown), reached a spike of $3.48 \text{ mg N}_2\text{O-N m}^{-2} \text{ h}^{-1}$ 48 hours after manure application, then
196 dropped to a minimum of $1.02 \text{ mg N}_2\text{O-N m}^{-2} \text{ h}^{-1}$ on 5 April. A maximum emission peak of
197 $3.55 \text{ mg N}_2\text{O-N m}^{-2} \text{ h}^{-1}$ was measured on 16 April and was most likely related to fertilizer
198 application.



199

200 **3.2 Comparison of the two emission techniques**

201 We selected the concurrent measurements from FG and the chambers and a total of 23
202 comparison pairs were obtained during the study period (note that each chamber observation
203 is an average from four replicate chambers). We calculated the ratio $Q_{FG}/Q_{chamber}$ of these
204 concurrent pairs.

205

206 The $Q_{FG}/Q_{chamber}$ ratio showed large variation, with values ranging between 0.4 and 4.9. The
207 $Q_{FG}/Q_{chamber}$ data follows a non-normal distribution. To better interpret these data we log-
208 transformed the ratios (Abdi et al., 2015). The average of the natural logarithm of the ratio,
209 converted back to the ratio units, gives the geometric mean (the process was duplicated to
210 calculate the confidence interval $\alpha = 0.9$). The geometric mean of $Q_{FG}/Q_{chamber}$ was 1.40, with
211 a confidence interval ranging from 1.15 to 1.69. This means that on average the FG measured
212 fluxes were 40% higher than those from the chambers, and this difference was statistically
213 significant.

214

215 Differences between chamber and micrometeorological measurements have been previously
216 noted. Some studies have reported that micrometeorological techniques gave emission rates
217 that were 50–60% of those from chambers (Christensen et al., 1996; Nefel et al., 2010). In
218 contrast, Wang et al. (2013) reported N_2O emissions measured by chambers were 17–20%
219 lower than from the eddy covariance micrometeorological technique, and Norman et al. (1997)
220 reported that chamber measurements were 30% lower than micrometeorological
221 measurements. Sommer et al. (2004) found static vented chambers underestimated N_2O
222 emissions from manure piles by 12–22% compared to mass balance measurements.

223



224 Discrepancies between FG and chamber fluxes could be due to very different measurement
225 footprints. Large spatial variability is a characteristic of soil N₂O emissions. For example,
226 Turner et al. (2008) reported N₂O emissions varied from 30 to 800 ng N₂O–N m⁻² s⁻¹ over an
227 irrigated dairy pasture (8,100 m²). This high variability, together with the substantial difference
228 in measurement footprint size (chambers < 1 m² vs FG > 1000 m²) will likely result in
229 differences between the two techniques because the chambers are not capable of accounting
230 for this variability, unless many chambers are used, whilst the FG method can. If this explains
231 the difference between the two techniques, then discrepancies between chambers and
232 micrometeorological techniques should be site dependent, i.e., dependent on the degree of
233 spatial variability in emissions at each site.

234

235 Several researchers have reported that chamber procedures introduced large uncertainty in N₂O
236 emissions (Levy et al., 2011; Venterea et al., 2010). In particular, using linear regression to
237 determine the rate of change dC/dt in Eq. (1) can lead to an underestimate of emissions
238 (Anthony et al., 1995; Matthias et al., 1978). Venterea (2013) concluded that the typical
239 calculations used for non-steady state chambers underestimated N₂O emissions by 20–50%.
240 Our results are in-line with this conclusion.

241

242 While there is a long and successful history of FG applications, there are still questions about
243 its implementation. The value of the turbulent Schmidt number (S_c) in Eq. (2) is debated (Flesch
244 et al., 2002). In addition, concerns about FG arise if the fetch (upwind distance from the
245 concentration measurement to the source edge) is not large. In our case the ratio of z_1 (the
246 maximum height of the OP-FTIR measurement path, 1.8 m) to the upwind fetch (minimum of
247 90–68 m for Sites 1 and 2, respectively) was < 1:35. This is considered to be sufficient in most
248 conditions, but during stable night-time conditions the fetch may not have been large enough



249 to satisfy the FG assumption of a constant flux layer (Flesch et al., 2016). In this case the FG
250 measurements would have been contaminated by emissions occurring upwind of our sites.
251 There is also a concern regarding the accuracy of FG during light winds. In our study the light
252 wind data ($0.05\text{--}0.15\text{ m s}^{-1}$) accounted for 24% of the measurement periods. We found the FG
253 uncertainty ($\delta_{Q_{FG}}/Q_{FG}$) increased from 0.41 to 1.25 when the friction velocity (u^*) dropped from
254 0.15 to 0.05 m s^{-1} . However, we note that in this study the periods in which we compared FG
255 and chamber measurements were not light wind periods.

256

257 **4 Conclusions**

258 Our results showed that FG and static chamber measurements of soil N_2O emissions were
259 statistically different, with fluxes from FG being on average 40% higher. Given the likelihood
260 of large spatial variability in N_2O emissions, and the vastly different measurement footprints
261 of the two methods, it is not surprising the two techniques give different results. It is difficult
262 to conclude that one technique or the other is biased based on this experiment alone. However,
263 the relationship we observed, together with other reports on the biases created by chamber
264 calculation procedures, supports an interpretation that our FG emission calculations were
265 accurate and in this instance the chamber measurements were biased too low.

266

267 The OP-FTIR flux gradient system used here showed the capability for real-time emission
268 measurements over a large spatial footprint with no surface interference. Furthermore, being
269 free from pumps and tubing, the open-path FG system would be particularly advantageous for
270 measuring multiple gas emissions including “sticky” gases like NH_3 .

271

272 **5 Author contribution**



273 DC, HS, SKL, MB and TF designed the experiments and MB and SKL carried them out. TF
274 and MB developed the techniques. MB prepared the manuscript with contributions from all
275 co-authors.

276

277 **6 Competing interests**

278 The authors declare that they have no conflict of interest.

279

280 **7 Acknowledgments**

281 This study was funded by the Australian Department of Agriculture (DA), and the Canadian
282 Agricultural Greenhouse Gases Program (AGGP). The authors thank Schruers' vegetable farm,
283 Adam Schruers and staff for their great support. The authors also thank Rohan Davies from
284 BASF Australia Ltd. for providing assistance. We gratefully acknowledge the assistance of the
285 staff and students from Faculty of Veterinary and Agricultural Sciences soil research group at
286 the University of Melbourne during this campaign. The valuable comments from three
287 unknown reviewers were appreciated.

288

289 **References**

290 Abdi, D., Cade-Menun, B.J., Ziadi, N., Parent, L.-É., 2015. Compositional statistical analysis
291 of soil ³¹P-NMR forms. *Geoderma*. 257–258, 40-47.

292 Anthony, W.H., Hutchinson, G.L., Livingston, G.P., 1995. Chamber measurement of soil-
293 atmosphere gas exchange: Linear vs. diffusion-based flux models. *Soil Sci. Soc. Am. J.* 59,
294 1308-1310.

295 Bai, M., 2010. Methane emissions from livestock measured by novel spectroscopic
296 techniques, School of Chemistry. University of Wollongong, p. 303.

297 Christensen, S., Ambus, P., Arah, J.R.M., Clayton, H., Galle, B., Griffith, D.W.T.,
298 Hargreaves, K.J., Klemmedtsson, L., Lind, A.M., Maag, M., Scott, A., Skiba, U., Smith, K.A.,
299 Welling, M., Wienhold, F.G., 1996. Nitrous oxide emission from an agricultural field:
300 comparison between measurements by flux chamber and micrometeorological techniques.
301 *Atmos. Environ.* 30, 4183.



- 302 Dalal, R.C., Allen, D.E., Livesley, S.J., Richards, G., 2008. Magnitude and biophysical
303 regulators of methane emission and consumption in the Australian agricultural, forest, and
304 submerged landscapes: a review. *Plant Soil*. 309, 43-76.
- 305 de Klein, C.A.M., Sherlock, R.R., Cameron, K.C., van der Weerden, T.J., 2001. Nitrous
306 oxide emissions from agricultural soils in New Zealand—A review of current knowledge and
307 directions for future research. *J. Roy. Soc. New Zeal.* 31, 543-574.
- 308 Denmead, O.T., 1979. Chamber systems for measuring nitrous oxide emission from soils in
309 the field. *Soil Sci. Soc. Am. J.* 43, 89-95.
- 310 Denmead, O.T., 1995. Novel meteorological methods for measuring trace gas fluxes. *Philos.*
311 *T. R. Soc. A.* 351, 383-396.
- 312 Denmead, O.T., 2008. Approaches to measuring fluxes of methane and nitrous oxide between
313 landscapes and the atmosphere. *Plant and Soil*. 309, 5-24.
- 314 Denmead, O.T., Chen, D., Griffith, D.W.T., Loh, Z.M., Bai, M., Naylor, T., 2008. Emissions
315 of the indirect greenhouse gases NH_3 and NO_x from Australian beef cattle feedlots. *Aust. J.*
316 *Exp. Agr.* 48, 213-218.
- 317 Denmead, O.T., Macdonald, B.C.T., Bryant, G., Naylor, T., Wilson, S., Griffith, D.W.T.,
318 Wang, W.J., Salter, B., White, I., Moody, P.W., 2010. Emissions of methane and nitrous
319 oxide from Australian sugarcane soils. *Agric. Forest Meteorol.* 150, 748-756.
- 320 Flesch, K.T., Baron, V., Wilson, J., Griffith, D.W.T., Basarab, J., Carlson, P., 2016.
321 Agricultural gas emissions during the spring thaw: Applying a new measurement technique.
322 *Agric. Forest Meteorol.* 221, 111-121.
- 323 Flesch, T.K., McGinn, S.M., Chen, D.L., Wilson, J.D., Desjardins, R.L., 2014. Data filtering
324 for inverse dispersion emission calculations. *Agric. Forest Meteorol.* 198-199, 1-6.
- 325 Flesch, T.K., Prueger, J.H., Hatfield, J.L., 2002. Turbulent Schmidt number from a tracer
326 experiment. *J. Appl. Meteorol.* 111, 299-307.
- 327 Griffith, D.W.T., 1996. Synthetic calibration and quantitative analysis of gas-phase FT-IR
328 spectra. *Appl. Spectrosc.* 50, 59-70.
- 329 Griffith, D.W.T., Deutscher, N.M., Caldow, C., Kettlewell, G., Riggensbach, M., Hammer, S.,
330 2012. A Fourier transform infrared trace gas and isotope analyser for atmospheric
331 applications. *Atmos. Meas. Tech.* 5, 2481-2498.
- 332 Griffith, D.W.T., Galle, B., 2000. Flux measurements of NH_3 , N_2O and CO_2 using dual beam
333 FTIR spectroscopy and the flux gradient technique. *Atmos. Environ.* 34, 1087-1098.
- 334 Hargreaves, K.J., Wienhold, F.G., Klemetsson, L., Arah, J.R.M., Beverland, I.J., Fowler, D.,
335 Galle, B., Griffith, D.W.T., Skiba, U., Smith, K.A., Welling, M., Harris, G.W., 1996.
336 Measurement of nitrous oxide from Agricultural land using micrometeorological methods.
337 *Atmos. Environ.* 30, 1563-1571.
- 338 Hutchinson, G.L., Mosier, A.R., 1981. Improved soil cover method for field measurement of
339 nitrous oxide fluxes. *Soil Sci. Soc. Am. J.* 45, 311-316.



- 340 Jones, S.K., Famulari, D., Di Marco, C.F., Nemitz, E., Skiba, U.M., Rees, R.M., Sutton,
341 M.A., 2011. Nitrous oxide emissions from managed grassland: a comparison of eddy
342 covariance and static chamber measurements. *Atmos. Meas. Tech.* 4, 2179-2194.
- 343 Judd, M.J., Kellier, F.M., Ulyatt, M.J., Lassey, K.R., Tate, K.R., Shelton, D., Harvey, M.J.,
344 Walker, C.F., 1999. Net methane emissions from grazing sheep. *Global Change Biol.* 5, 647-
345 657.
- 346 Laubach, J., Kelliher, F.M., 2004. Measuring methane emission rates of a dairy cow herd by
347 two micrometeorological techniques. *Agric. Forest Meteorol.* 125, 279-303.
- 348 Levy, P.E., Gray, A., Leeson, S.R., Gaiawyn, J., Kelly, M.P.C., Cooper, M.D.A., Dinsmore,
349 K.J., Jones, S.K., Sheppard, L.J., 2011. Quantification of uncertainty in trace gas fluxes
350 measured by the static chamber method. *Eur. J. Soil Sci.* 62, 811-821.
- 351 Li, J., Tong, X., Yu, Q., Dong, Y., Peng, C., 2008. Micrometeorological measurements of
352 nitrous oxide exchange above a cropland. *Atmos. Environ.* 42, 6992-7001.
- 353 Matthias, A.D., Yarger, D.N., Weinback, R.S., 1978. A numerical evaluation of chamber
354 methods for determining gas fluxes. *Geophys. Res. Lett.* 5, 765-768.
- 355 Neftel, A., Ammann, C., Fischer, C., Spirig, C., Conen, F., Emmenegger, L., Tuzson, B.,
356 Wahlen, S., 2010. N₂O exchange over managed grassland: Application of a quantum cascade
357 laser spectrometer for micrometeorological flux measurements. *Agric. Forest Meteorol.* 150,
358 775-785.
- 359 Norman, J.M., Kucharik, C.J., Gower, S.T., Baldocchi, D.D., Crill, P.M., Rayment, M.,
360 Savage, K., Striegl, R.G., 1997. A comparison of six methods for measuring soil-surface
361 carbon dioxide fluxes. *J. Geophys. Res.* 102, 28771-28777.
- 362 Pattey, E., Strachan, I.B., Desjardins, R.L., Edwards, G.C., Dow, D., MacPherson, J.I., 2006.
363 Application of a tunable diode laser to the measurement of CH₄ and N₂O fluxes from field to
364 landscape scale using several micrometeorological techniques. *Agric. Forest Meteorol.* 136,
365 222-236.
- 366 Ruser, R., Flessa, H., Schilling, R., Steindl, H., Beese, F., 1998. Soil compaction and
367 fertilization effects on nitrous oxide and methane fluxes in potato fields. *Soil Sci. Soc. Am. J.*
368 62, 1587-1595.
- 369 Sommer, S.G., McGinn, S.M., Hao, X., Larney, F.J., 2004. Techniques for measuring gas
370 emissions from a composting stock pile of cattle manure. *Atmos. Environ.* 38, 4643-4652.
- 371 Turner, D.A., Chen, D., Galbally, I.E., Leuning, R., Edis, R.B., Li, Y., Kelly, K., Phillips, F.,
372 2008. Spatial variability of nitrous oxide emissions from an Australian irrigated dairy pasture.
373 *Plant and Soil.* 309, 77-88.
- 374 Venterea, R.T., 2013. Theoretical comparison of advanced methods for calculating nitrous
375 oxide fluxes using non-steady state chambers. *Soil Sci. Soc. Am. J.* 77, 709-720.
- 376 Venterea, R.T., Dolan, M., Ochsner, T.E., 2010. Urea decreases nitrous oxide emissions
377 compared with anhydrous ammonia in a Minnesota corn cropping system. *Soil Sci. Soc. Am.*
378 *J.* 74, 407-418.



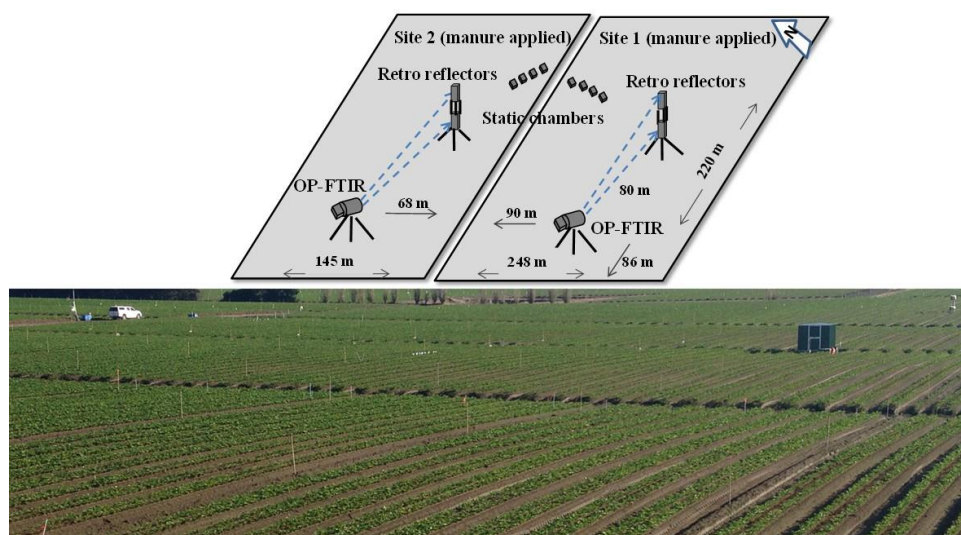
- 379 Wang, K., Zheng, X., Pihlatie, M., Vesala, T., Liu, C., Haapanala, S., Mammarella, I.,
380 Rannik, Ü., Liu, H., 2013. Comparison between static chamber and tunable diode laser-based
381 eddy covariance techniques for measuring nitrous oxide fluxes from a cotton field. *Agric.*
382 *Forest Meteorol.* 171–172, 9-19.
- 383 Webb, E.K., Pearman, G.I., Leuning, R., 1980. Correction of flux measurements for
384 chemistry effects due to heat and water vapour transfer. *Quart. J. R. Meteorol. Soc.* 106, 85-
385 100.
- 386 Wilson, J.D., Flesch, T.K., 2016. Generalized flux-gradient technique pairing line-average
387 concentrations on vertically separated paths. *Agric. Forest Meteorol.* 220, 170-176.
- 388 Yao, Z., Zheng, X., Xie, B., Liu, C., Mei, B., Dong, H., Butterbach-Bahl, K., Zhu, J., 2009.
389 Comparison of manual and automated chambers for field measurements of N₂O, CH₄, CO₂
390 fluxes from cultivated land. *Atmos. Environ.* 43, 1888-1896.

391

392 Figures

393 Figure 1

394



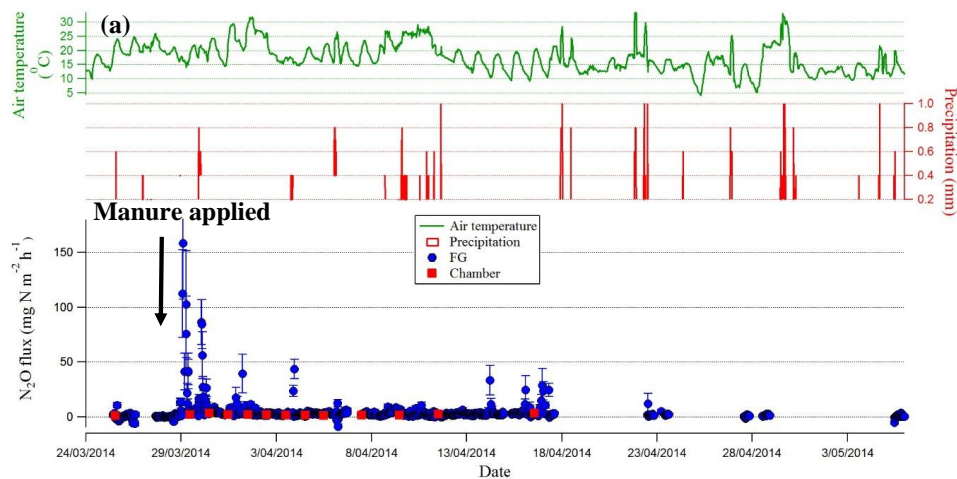
395

396 **Figure 1** The design of the study (upper panel) and photo of experimental site with OP-FTIR
397 set up (lower panel). Emission measurements were conducted with static chambers (four per
398 site) and FG using the OP-FTIR spectroscopy system with retro reflectors at 0.8 and 1.8 m
399 above ground. The figure is not in scale.

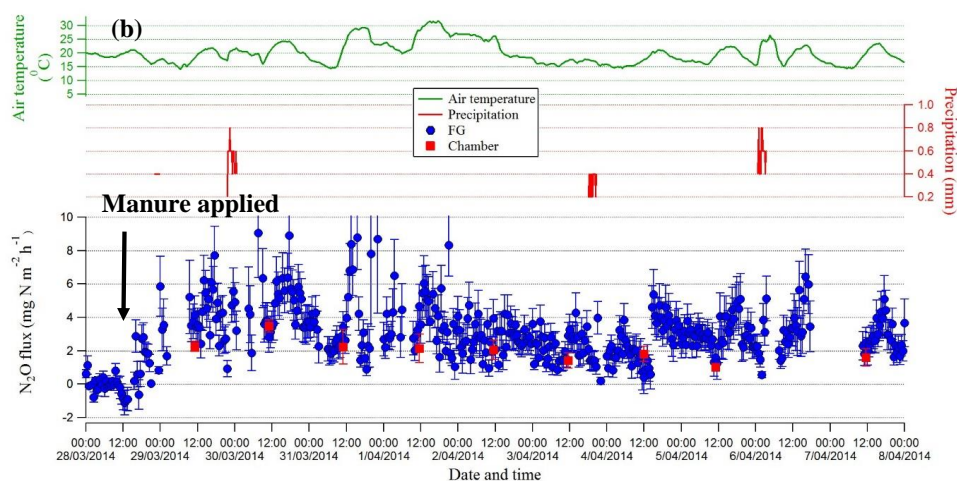


400

401 Figure 2



402



403

404 **Figure 2** (a) Hourly N_2O fluxes measured by FG and static chambers from 25 March to 6 May.

405 Air temperature and precipitation are plotted during the same period; and (b) subset of N_2O

406 fluxes from 28 March to 8 April. Error bars (both upper and lower panels) represent $1-\sigma$

407 estimate of measurement uncertainty (δ_{QFG}) for the FG measurements and standard error for

408 chambers. Manure was applied on 28 March 2014.